Acta Crystallographica Section B
Structural Science
ISSN 0108-7681

Isostructuralism in a series of methylester/methylamide derivatives of (*R*,*R*)-*O*,*O*′-dibenzoyl tartaric acid; inclusion properties and guest-dependent homeotypism of the crystals of (*R*,*R*)-*O*,*O*′-dibenzoyltartaric acid diamide

Urszula Rychlewska* and Beata Warżajtis

Department of Crystallography, Faculty of Chemistry, Adam Mickiewicz University, Grunwaldzka 6, 60-780 Poznań, Poland

Correspondence e-mail: urszular@amu.edu.pl

Received 9 October 2001
Accepted 12 November 2001

The compounds studied are methyl ester, amide and methylamide derivatives of (*R*,*R*)-*O*,*O*′-dibenzoyl tartaric acid. The molecules adopt the planar *T* conformation of the four-carbon chain with the terminal C═O bonds situated *antiperiplanar* with respect to the nearest C*—O bond. All investigated molecules occupy a twofold symmetry site in the crystal, including the mono(*N*-methylamide) monomethylester which lacks the C_2 molecular symmetry. Connected with this is the static disorder in which the methylester and the *N*-methylamide groups replace each other and isostructuralism within the methylester/methylamide series. (*R*,*R*)-*O*,*O*′-Dibenzoyltartaric acid diamides [(*R*,*R*)-*O*,*O*′-dibenzoyl-2,3-dihydroxybutanediamides], both primary and secondary, form hydrogen-bond aggregation patterns typical for amides, despite the presence of other hydrogen-bond acceptors in the molecule. However, in primary amides such packing leads to the creation of homeotypic crystal structures in which structural voids are filled by cyclic solvent molecules (pyridine, 1,4-dioxane). The presence of polyamide ladders, consisting of 'fused' hydrogen-bond rings, seems to be responsible for the low solubility and high melting point of these substances.

1. Introduction

Although the role of tartaric acid, its derivatives and salts in the development of the fundamental concepts of organic stereochemistry has long been recognized, it was only recently that its potential use in supramolecular chemistry has been acknowledged. This symmetrical and highly functionalized molecule can be modified by substitution to obtain molecules and crystals of desired properties. For example, (*R*,*R*)-*O*,*O*′-dibenzoyl tartaric acid, besides being known as an excellent resolving agent for racemic amines and acid hydrazides *via* their diastereomeric salts (Gawroński & Gawrońska, 1999), has been shown to possess the crystalline inclusion properties (Szczepańska *et al.*, 1995) which can be used for the resolution of non-basic racemates (Kozma *et al.*, 1996). Interestingly, the parent tartaric acid molecule does not form molecular complexes. It seems as though to display inclusion properties a partial rigidification of this seemingly flexible molecule is desired and this can be readily obtained by dibenzoylation. In line with this statement is our recent discovery that (*R*,*R*)-*O*,*O*′-dibenzoyltartaric acid diamide also displays inclusion properties which are reported in this paper together with the results obtained for the closely related structures that constitute a series of methylester and *N*-methylamide derivatives. The paper is a continuation of our previous studies on conformational preferences and the mode of molecular asso-

Table 1
The structures discussed.

Abbreviations: numbers 1 and 2 designate primary and secondary amide substituents, respectively, while OM represents methyl ester substituents; B represents the benzoylated derivatives

	X	*Y*	Abbreviation
Dimethyl (*R*,*R*)-(−)-*O*,*O*′-dibenzoyltartrate	OMe	OMe	BOM
(*R*,*R*)-(−)-*O*,*O*′-Dibenzoyltartaric acid *N*,*N*′-dimethyldiamide	NHMe	NHMe	BN22
(*R*,*R*)-(−)-*O*,*O*′-Dibenzoyltartaric acid mono(*N*-methylamide) monomethylester	OMe	NHMe	BOM2
(*R*,*R*)-(−)-*O*,*O*′-Dibenzoyltartaric acid diamide	NH_2	NH_2	BN11

ciation of covalent derivatives of optically active tartaric acid, namely esters, amides, *N*-methylamides and *N*,*N*′-dimethylamides and their dibenzoyl derivatives (Gawroński *et al.*, 1989, 1997; Rychlewska *et al.*, 1997, 1999; Rychlewska & Warżajtis, 2000, 2001; Szarecka *et al.*, 1996, 1999, 2000; Szczepańska & Rychlewska, 1994).

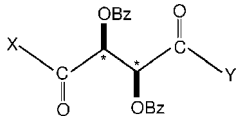

2. Experimental

2.1. Synthesis

The investigated compounds, presented in Table 1, have been obtained in the Department of Organic Stereochemistry (formerly the Laboratory of Natural Products), Faculty of Chemistry, Adam Mickiewicz University, Poznań, Poland (Gawroński *et al.*, 1997).

2.2. X-ray crystallography

Reflection intensities for compounds listed in Table 1 were measured at room temperature on a four-circle Syntex $P2_1$ and KM-4 Kuma Diffraction diffractometers or on a Kuma CCD diffractometer at 160 K. The diffractometers were equipped with graphite monochromators. The background and integrated intensities for reflections measured on a Syntex diffractometer were evaluated from a profile analysis according to Lehmann & Larsen (1974) using the program *PRARA* (Jaskólski, 1982). The intensities were corrected for Lorentz and polarization effects. The structures were solved by direct methods with *SHELXS*86 (Sheldrick, 1990) and refined against F^2 with *SHELXL*97 (Sheldrick, 1997). Non-H atoms (C, O, N) were refined anisotropically. The positions of the H atoms were calculated and refined using a riding model and their isotropic displacement parameters were given a value 20% higher than the isotropic equivalent for the atom to which the H atom was bonded. The 1,4-dioxane molecule included in the crystal lattice of BN11 was found to be disordered over two alternative orientations, generated by the twofold axis. Similarly, in the crystal structure of BOM2 the methylester and methylamide groups situated at both ends of the molecule display static disorder connected with the fact that the molecule occupies the twofold symmetry site. Accordingly, the disorder was modelled with occupancy factors of 0.5 for both cases. Crystals of BOM2 were poorly diffracting; therefore, to improve the quality of the diffraction pattern we have performed the intensity measurements at 160 K on the biggest available crystal. The absolute structure of the crystals was assumed from the known absolute configuration of the reagents used in the synthesis. A Siemens Stereochemical Workstation (Siemens, 1989) was used to prepare the drawings. Crystal data and details of data collection and structure refinement are summarized in Table 2.[1]

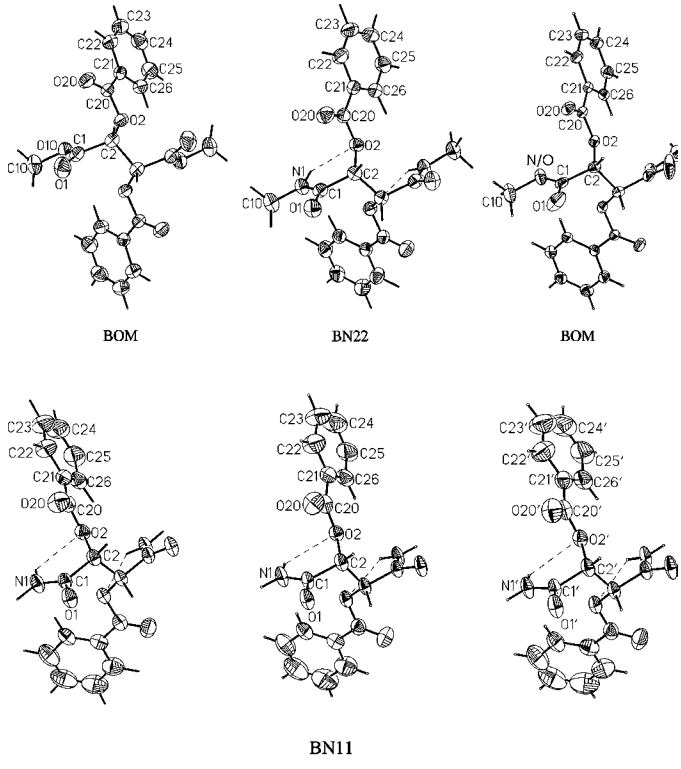

Figure 1
*ORTEP*II (Johnson, 1976) drawing of the investigated molecules with atom-numbering scheme. Thermal ellipsoids are drawn at 40% probability level. All molecules occupy a twofold symmetry site in the crystal. In BOM2, which lacks the C_2 symmetry, both the ester oxygen and the amide nitrogen occupy the same site, with s.o.f. 0.5 (the amide hydrogen has been omitted). All three molecules of BN11 (two in a complex with pyridine and one in a complex with 1,4-dioxane) are shown to illustrate that they are virtually equal. Intramolecular hydrogen bonds have been marked with dashed lines.

[1] Supplementary data for this paper are available from the IUCr electronic archives (Reference: NA0128). Services for accessing these data are described at the back of the journal.

Table 2
Experimental details.

	BN11·1,4-dioxane	BN11·pyridine	BOM	BN22	BOM2
Crystal data					
Chemical formula	$C_{18}H_{16}N_2O_6·C_4H_8O_2$	$C_{18}H_{16}N_2O_6·C_5H_5N$	$C_{20}H_{18}O_8$	$C_{20}H_{20}N_2O_6$	$C_{20}H_{19}NO_7$
Chemical formula weight	444.43	435.43	386.34	384.38	385.36
Cell setting, space group	Orthorhombic, $C222_1$	Monoclinic, $C2$	Orthorhombic, $P2_12_12$	Orthorhombic, $P2_12_12$	Orthorhombic, $P2_12_12$
a, b, c (Å)	5.253 (1), 26.748 (5), 15.621 (3)	27.898 (6), 5.145 (1), 15.648 (3)	9.462 (1), 17.653 (3), 5.662 (1)	10.282 (2), 18.024 (4), 5.136 (1)	9.898 (2), 17.756 (4), 5.264 (1)/9.94 (1), 17.95 (2), 5.341 (0)
β (°)	90	93.49 (3)	90	90	90
V (Å^3)	2194.9 (7)	2241.9 (8)	945.7 (3)	951.8 (3)	925.1 (3)/952 (3)
Z	4	4	2	2	2
D_x (Mg m^{-3})	1.345	1.290	1.357	1.341	1.383
Radiation type	Cu $K\alpha$	Cu $K\alpha$	Cu $K\alpha$	Mo $K\alpha$	Mo $K\alpha$
No. of reflections for cell parameters	51	53	15	15	3407
θ range (°)	12.22–23.58	12.04–24.98	6–17	10.54–14.20	–
μ (mm^{-1})	0.870	0.789	0.897	0.100	0.106
Temperature (K)	293 (2)	293 (2)	293 (2)	293 (2)	160 (2)
Crystal form, colour	Plate, colourless	Needle, colourless	Needle, colourless	Plate, colourless	Needle, colourless
Crystal size (mm)	0.40 × 0.30 × 0.05	0.60 × 0.12 × 0.08	0.50 × 0.40 × 0.30	0.50 × 0.40 × 0.30	0.70 × 0.15 × 0.15
Data collection					
Diffractometer	KM-4 four circle	KM-4 four circle	Syntex $P2_1$	Syntex $P2_1$	Kuma KM-4 CCD κ geometry
Data collection method	θ–2θ scans	θ–2θ scans	θ–2θ scans	θ–2θ scans	ω scans
No. of measured, independent and observed parameters	1886, 1795, 1410	3629, 3559, 1994	783, 783, 758	1097, 1097, 798	3976, 976, 966
Criterion for observed reflections	$I > 2\sigma(I)$	$I > 2\sigma(I)$	$I > 2\sigma(I)$	$I > 2\sigma(I)$	$I > 2\sigma(I)$
R_{int}	0.0218	0.0425	0.0000	0.0000	0.0594
θ_{max} (°)	65.15	64.81	57.23	26.06	25.00
Range of h, k, l	$-5 \rightarrow h \rightarrow 5$ $0 \rightarrow k \rightarrow 31$ $0 \rightarrow l \rightarrow 18$	$-32 \rightarrow h \rightarrow 32$ $-6 \rightarrow k \rightarrow 6$ $0 \rightarrow l \rightarrow 18$	$-10 \rightarrow h \rightarrow 0$ $-19 \rightarrow k \rightarrow 0$ $-6 \rightarrow l \rightarrow 0$	$-12 \rightarrow h \rightarrow 0$ $-22 \rightarrow k \rightarrow 0$ $-6 \rightarrow l \rightarrow 0$	$-11 \rightarrow h \rightarrow 11$ $-21 \rightarrow k \rightarrow 21$ $-6 \rightarrow l \rightarrow 3$
No. and frequency of standard reflections	2 every 100 reflections	2 every 100 reflections	2 every 100 reflections	3 every 100 reflections	–
Intensity decay (%)	2.15	0.42	2.03	3.57	–
Refinement					
Refinement on	F^2	F^2	F^2	F^2	F^2
$R[F^2>2\sigma(F^2)]$, $wR(F^2)$, S	0.0485, 0.1392, 1.062	0.0459, 0.1389, 1.002	0.0252, 0.0718, 1.146	0.0452, 0.135, 1.083	0.0832, 0.1679, 1.135
No. of reflections and parameters used in refinement	1795, 173	3559, 290	783, 129	1097, 128	976, 128
H-atom treatment	Riding model	Riding model	Riding model	Riding model	Riding model
Weighting scheme	$w = 1/[\sigma^2(F_o^2) + (0.0893P)^2 + 0.2101P]$, where $P = (F_o^2 + 2F_c^2)/3$	$w = 1/[\sigma^2(F_o^2) + (0.0746P)^2 + 0.0000P]$, where $P = (F_o^2 + 2F_c^2)/3$	$w = 1/[\sigma^2(F_o^2) + (0.0428P)^2 + 0.1101P]$, where $P = (F_o^2 + 2F_c^2)/3$	$w = 1/[\sigma^2(F_o^2) + (0.0827P)^2 + 0.1003P]$, where $P = (F_o^2 + 2F_c^2)/3$	$w = 1/[\sigma^2(F_o^2) + (0.0000P)^2 + 3.2945P]$, where $P = (F_o^2 + 2F_c^2)/3$
$(\Delta/\sigma)_{max}$	0.000	0.000	0.000	0.000	0.000
$\Delta\rho_{max}$, $\Delta\rho_{min}$ (e Å^{-3})	0.241, −0.179	0.186, −0.165	0.125, −0.093	0.162, −0.166	0.303, −0.282
Extinction method	*SHELXL*	*SHELXL*	*SHELXL*	*SHELXL*	*SHELXL*
Extinction coefficient	0.0020 (4)	0.0021 (2)	0.0191 (15)	0.029 (8)	0.014 (6)

Computer programs used: Kuma *KM*-4 software (Kuma Diffraction, 1991), *DATAPROC* (Gałdecki *et al.*, 1995), *SHELXS*86 (Sheldrick, 1990), *SHELXL*97 (Sheldrick, 1997), Syntex Operation Manual, Syntex *XTL* Operation Manual, *PRARA*, Kuma *KM*-4 CCD software (Kuma Diffraction, 1999*a*,*b*).

3. Results and discussion

3.1. Molecular conformation

A perspective view of the investigated molecules showing their conformation and numbering system is given in Fig. 1. All but one (BOM2) of the molecules reported in this paper possess the C_2 symmetry, but all occupy the twofold symmetry site in the crystal lattice. Similarly to their parent compound, the optically active tartaric acid, all molecules adopt the staggered conformation, with a planar carbon chain and with the amide or methylester groups in *trans* (*T*) orientation with respect to each other (Fig. 1, Table 3). The *T* conformer has

Table 3
Selected torsion angles (°).

	C1—C2—C2A—C1*A*	O1═C1—C2—O2	H2—C2—O2—C20	C2—O2—C20═O20	O20═C20—C21—C22
BOM	166.3 (3)	−167.4 (2)	−49	−4.2 (3)	4.5 (3)
BN22	−178.0 (4)	−156.5 (3)	−42	−14.4 (4)	−4.2 (6)
BOM2	172.1 (8)	−164.0 (6)	−44	−8.7 (8)	−2.3 (9)
BN11·pyridine	−179.4 (4)	−157.2 (3)	−43	−13.1 (5)	−8.0 (7)
	−179.0 (4)	−153.8 (4)	−47	−11.0 (5)	−11.3 (7)
BN11·1,4-dioxane	−179.6 (4)	−158.1 (2)	−42	−12.3 (4)	−6.8 (5)

both C*—O(Bz) bonds situated nearly in-plane of the proximal amide or ester groups, despite the presence or absence of intramolecular hydrogen bonds that could stabilize this conformation (Fig. 1). A similar trend has been observed in a series of unsymmetrically substituted derivatives of (*R*,*R*)-*O*,*O*′-dibenzoyl tartaric acid (Rychlewska & Warżajtis, 2001), as well as in the analogous series of non-benzoylated derivatives (Rychlewska & Warżajtis, 2000). In the reported symmetrically substituted derivatives of (*R*,*R*)-*O*,*O*′-dibenzoyl tartaric acid, deviations from planarity seem more pronounced than in the non-benzoylated series (Rychlewska & Warżajtis, 2000), but are still less severe than in some unsymmetrically substituted dibenzoylated derivatives (Rychlewska & Warżajtis, 2001; Table 3). The deviations from planarity of the O═C—C*—O fragments seem to originate from the fact that the molecules utilize their molecular symmetry in the crystal which might be a source of additional strain introduced to the molecule. One of the consequences of the virtual planarity of both O═C—C*—O fragments is that the benzoyloxy carbonyl does not eclipse the nearest C*—H bond [the average H—C*—O—C torsion angle equals 44 (3)°, see Table 3). This observation is contrary to the assumptions usually

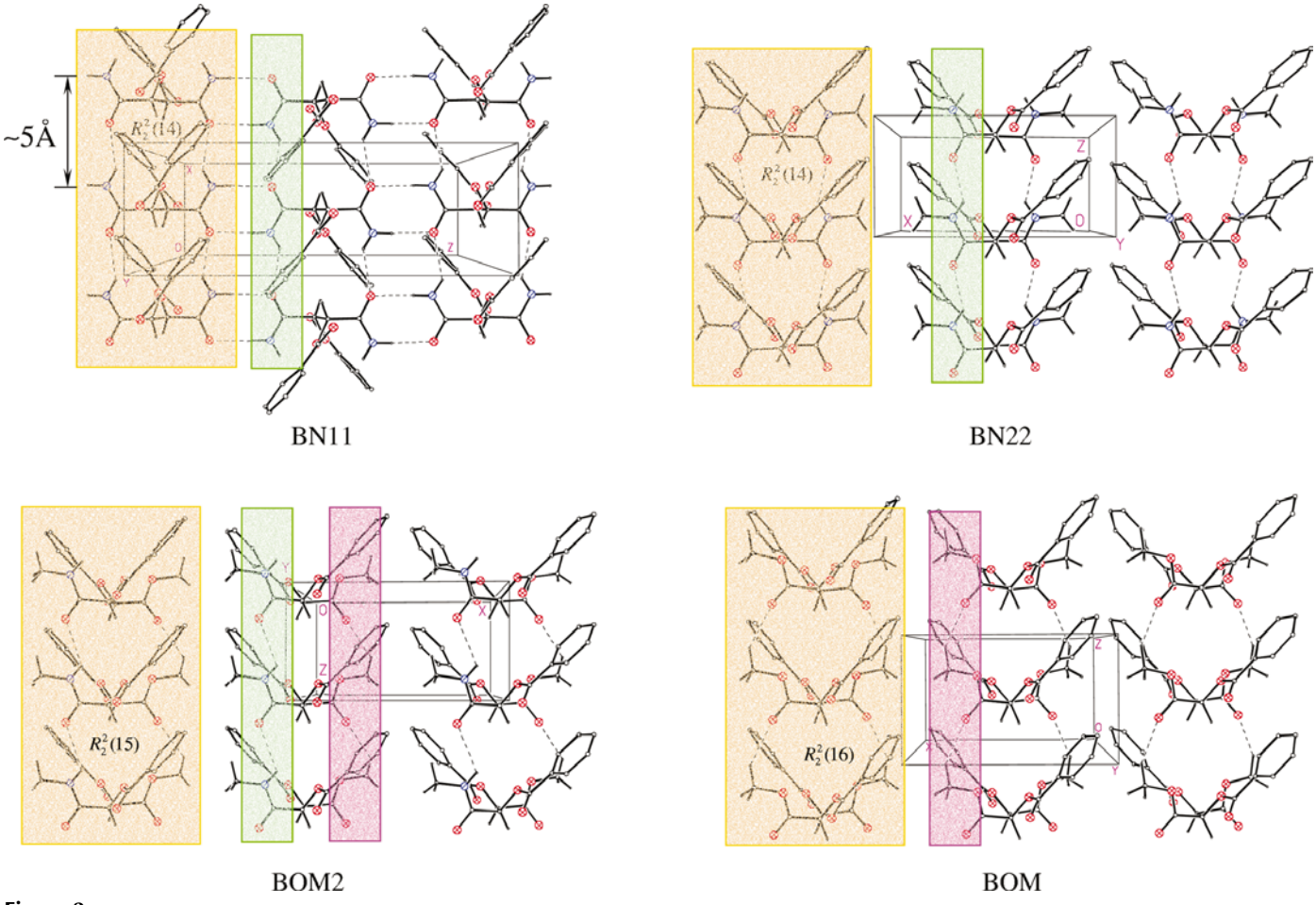

Figure 2
Arrangement of the investigated molecules in the crystal lattice (the H atoms of the phenyl rings have been omitted for clarity). Areas shaded in yellow illustrate polyamide ladders consisting of $R_2^2(14)$ rings, typical building blocks of primary and secondary (*R*,*R*)-*O*,*O*′-dibenzoyltartaric acid diamides (BN11, BN22) as well as the analogous ladders, consisting of $R_2^2(15)$ and $R_2^2(16)$ rings, formed in BOM2 and BOM, respectively. Areas shaded in green represent N—H···O═C amide hydrogen bonds (BN11, BN22, BOM2), while those shaded in pink illustrate their replacement, the weak C—H···O═C interactions (BOM2, BOM).

Table 4
Hydrogen-bond geometry of the *O*,*O*′-dibenzoyl derivatives of (*R*,*R*)-tartaric acid, substituted by methylesters, amides and methylamides.

Intramolecular hydrogen bonds have been marked with asterisks; carbon···oxygen hydrogen bonds have been written in italic; C—H, N—H and O—H distances have been standardized to values 1.10, 1.03 and 0.97 Å, respectively.

Compound		*D*···*A* (Å)	H···*A* (Å)	*D*—H···*A* (°)	Symmetry operations on *A*
BOM	*C10—H103···O1*	*3.458 (4)*	*2.54*	*140*	$x, y, -1+z$
M = 386.34					
m.p. = 404–407 K					
BN22	N1—H1···O2*	2.808 (4)	2.39	103	
	N1—H1···O1	2.894 (4)	2.11	131	$x, y, 1+z$
M = 384.38	*C26—H26···O1*	*3.404 (5)*	*2.45*	*144*	$1-x, 1-y, 1+z$
m.p. = 540–542 K					
BOM2	N1—H1···O2*	2.700 (7)	2.28	103	
	N1—H1···O1	3.116 (10)	2.55	114	$x, y, -1+z$
M = 385.36	*C10—H102···O1*	*3.173 (12)*	*2.36*	*129*	$x, y, -1+z$
m.p. = 447–450 K	*C26—H26···O1*	*3.378 (8)*	*2.50*	*136*	$-2-x, -1-y, -1+z$
BN11·pyridine	N1—H12···O2*	2.781 (4)	2.40	100	
	N1′—H12′···O2′*	2.789 (4)	2.42	100	
M = 435.43	N1—H11···O1′	2.956 (4)	1.93	175	$-\frac{1}{2}-x, \frac{1}{2}+y, -1-z$
m.p. = 526–527 K	N1—H12···O1	2.922 (4)	2.13	132	$x, 1+y, z$
	N1′—H11′···O1	2.916 (4)	1.89	174	$-\frac{1}{2}-x, -\frac{1}{2}+y, -1-z$
	N1′—H12′···O1’	2.909 (4)	2.08	136	$x, -1+y, z$
	C26—H26···O1	*3.446 (6)*	*2.52*	*141*	$-x, 1+y, -1-z$
BN11·1,4 dioxane	N1—H12···O2*	2.771 (3)	2.39	101	
	N1—H11···O1	2.963 (3)	1.93	176	$-1-x, y, -\frac{1}{2}-z$
M = 444.34	N1—H12···O1	3.043 (3)	2.26	132	$-1+x, y, z$
m.p. = 523–525 K	*C24—H24···O4S*	*3.321 (10)*	*2.43*	*137*	$-\frac{1}{2}+x, -\frac{1}{2}-y, -1-z$
	C26—H26···O1	*3.411 (5)*	*2.52*	*138*	$-1+x, -1-y, -1-z$
	C2S—H2S1···O20	*3.267 (14)*	*2.23*	*156*	$-1+x, y, z$
	C6S—H6S2···O20	*3.280 (14)*	*2.52*	*126*	$-1-x, y, -\frac{1}{2}-z$

made when interpreting circular dichroism results (Gawroński *et al.*, 1997), that an eclipsed O═C—O—C*—H system should be expected. The benzoate group is planar or nearly planar; the $O{=}C{-}C_{phenyl}{-}C_{phenyl}$ torsion angles range from 2.3 (9) to 11.3 (7)° (Table 3). The dihedral angle formed by the phenyl substituents ranges from 73.02 (7) to 89.21 (16)°.

3.2. Isostructuralism in a series of methylester/methylamide derivatives of (*R*,*R*)-*O*,*O*′-dibenzoyl tartaric acid

Three of the studied compounds, BOM, BN22 and BOM2, form the isostructural series. The first two molecules possess twofold symmetry (C_2), which is maintained in the crystal; the third, the unsymmetrically substituted derivative (BOM2), also utilizes the twofold symmetry site in the crystal. The period along the twofold axis has the length of ∼5–6 Å (Table 2). In BN22 the molecules related by a single translation along the twofold axis form head-to-head hydrogen bonds in which the amide hydrogen situated *trans* to the amide carbonyl is a donor to a translationally related amide carbonyl oxygen. This leads to the formation of typical amide chains described by the $C(4)$ pattern designator (Bernstein *et al.*, 1995; Fig. 2[2]). Due to its twofold symmetry, one molecule participates in the formation of two such chains in which the hydrogen bonds run parallel. Consequently, each molecule is hydrogen bonded to two translationally equivalent neighbouring molecules and participates in four hydrogen bonds: twice as a donor and twice as an acceptor. In other words, each molecule belongs to two hydrogen-bond rings, sharing the common carbon chain, each described by the $R_2^2(14)$ motif. Ladder-type ribbons, consisting of such rings, extend in the direction of the 5 Å unit-cell side. This supramolecular motif can be considered as characteristic for primary and secondary linear diamides (Motherwell *et al.*, 2000; Fig. 2; BN11 BN22). It seems as though the necessary condition for the formation of polyamide ladders is that the molecule utilizes the twofold symmetry in the crystal and that this twofold axis has a unit length of approximately 5 Å. Consequently, asymmetric substitution might preclude formation of the $R_2^2(14)$ rings.

The packing pattern analogous to the one described above for BN22 is seen in the crystal structure of BOM (Fig. 2) and BOM2 and, what is more, these crystals are isostructural (Table 2). This phenomenon can be interpreted as an illustration of close topological similarity between methyl ester and methylamide groups. Since the methylester group does not possess the ‘classical’ hydrogen-bond donor, the role of the amide hydrogen bond is taken over by C(methyl)—H···O interactions which, in the case of BOM, means the replacement of $R_2^2(14)$ rings by $R_2^2(16)$ motifs (Fig. 2). The question arises as to whether the formation of the same pattern in the crystal structure is induced by close packing and similarity in size and shape of these molecules or by weak C(methyl)—

[2] The following symbols appear in Figs. 2 and 3: ○ H atoms, ○ C atoms, ◯ N atoms, ⊘ O atoms

H···O interactions that replace N—H···O hydrogen bonds (Table 4) or a combination of these two effects.

3.3. Inclusion properties of (*R*,*R*)-*O*,*O*′-dibenzoyltartaric acid diamide (BN11) resulting from the perfectly layered arrangement of hydrogen-bonded molecules

(*R*,*R*)-*O*,*O*′-Dibenzoyltartaric acid diamide forms lattice inclusion compounds with pyridine and 1,4-dioxane (Table 4, Fig. 3). The molecule possesses twofold symmetry (C_2) which is maintained in the crystal and extends along the crystallographic axis, along which the period is of ∼5 Å. The molecules related by a single translation along this axis are connected together by pairs of $NH_{trans}\cdots O{=}C$ hydrogen bonds. This leads to the formation of the parallel ladder pattern, consisting of the 'fused' $R_2^2(14)$ rings, which has already been described above. The second hydrogen, situated *cis* to the amide carbonyl group, is used to join neighbouring molecules into the amide $R_2^2(8)$ dimers (Figs. 2 and 3). The molecules forming the dimer are either related by the twofold axis (BN11·1,4-dioxane, space group $C222_1$) or are crystallographically independent (BN11·pyridine, space group $C2$). Otherwise, the two crystal structures are very much alike and therefore can be considered as homeotypic. The formation of amide dimers allows the parallel ladders described above to be joined by hydrogen bonds into layers in which neighbouring ladders are oriented antiparallel. The layers run perpendicular to the crystallographic axes, along which the repetition period amounts to approximately 27 Å (Table 2). In both crystal structures, consecutive layers are generated by the C-lattice translation which causes a mutual shift of the molecules in one layer with respect to the molecules in the consecutive layer along the shortest unit cell side (∼5 Å) by half of its parameter. A perfectly layered arrangement of hydrogen-bonded molecules creates structural voids around the $R_4^2(8)$ motif (Fig. 3), which are filled by organic solvents such as pyridine or dioxane.

The parallel ladders consisting of 'fused' $R_2^2(14)$ rings, either separated (as in BN22) or further joined into layers (as in BN11), seem to be responsible for exceptionally low solubility of dibenzoylated primary and secondary (*R*,*R*)-tartramides in common organic solvents such as alcohols, ethers and acetone, while they dissolve in DMSO, DMF, pyridine *etc*. The two types of crystal display very high melting points (Table 4), the highest among all derivatives studied (Rychlewska & Warżajtis, 2000, 2001).

4. Conclusions

Symmetrically substituted derivatives of (*R*,*R*)-*O*,*O*′-dibenzoyl tartaric acid tend to maintain their twofold symmetry in their crystals, a situation not observed in their non-benzoylated analogues. The molecules arrange in a head-to-head mode, with hydrogen bonds joining the molecules related by lattice translation. This is contrasted with the behaviour of unsymmetrical derivatives which arrange in a head-to-tail mode. Self-association of symmetrically substituted (*R*,*R*)-*O*,*O*′-dibenzoyltartramides follows the rules that govern the packing of amides in the solid state [the $C(4)$ and $R_2^2(8)$ motifs]. As a result we observe the formation of polyamide ladders and layers as well as the layer-induced inclusion phenomenon which may potentially be used for the resolution of racemates. The methylester substituent has the ability to isomorphously replace the *N*-methylamide fragment in the crystal lattice which, consequently, leads to the replacement of N—H···O by C—H···O hydrogen bonds. Isomorphism in the series of methylester/methylamide derivatives might originate from the favourable spatial arrangement, dictated by hydro-

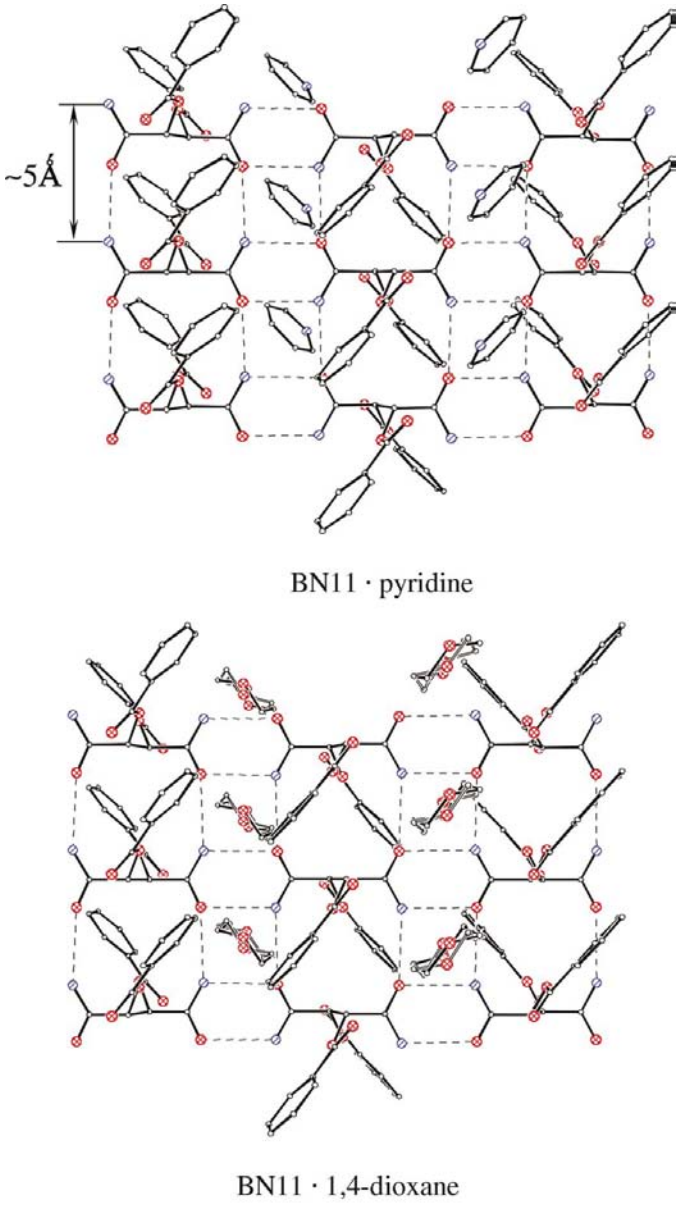

Figure 3
Guest-dependent homeotypism of (*R*,*R*)-*O*,*O*′-dibenzoyltartaric acid diamide (BN11) crystals. Layers of hydrogen-bonded molecules with solvent molecules located in voids formed around the $R_4^2(8)$ rings: BN11·pyridine, space group $C2$; BN11·1,4-dioxane, space group $C222_1$. The H atoms have been omitted for clarity.

phobic components, or might be interpreted as evidence of the presence of C—H···O hydrogen bonds in the crystalline state.

The authors wish to thank Professor J. Gawroński for providing the samples for X-ray analysis and for his stimulating interest in this work.

References

Bernstein, J., Davis, R. E., Shimoni, L. & Chang, N. L. (1995). *Angew. Chem. Int. Ed. Engl.* **34**, 1555–1573.

Gałdecki, Z., Kowalski, A. & Uszyński, L. (1995). *DATAPROC Data Processing Program*, Version 9. Kuma Diffraction, Wrocław, Poland.

Gawroński, J. & Gawrońska, K. (1999). *Tartaric and Malic Acids in Synthesis*. New York: John Wiley and Sons Inc.

Gawroński, J., Gawrońska, K. & Rychlewska, U. (1989). *Tetrahedron Lett.* **30**, 6071–6074.

Gawroński, J., Gawrońska, K., Skowronek, P., Rychlewska, U., Warżajtis, B., Rychlewski, J., Hoffmann, M. & Szarecka, A. (1997). *Tetrahedron*, **53**, 6113–6144.

Jaskólski, M. (1982). *Collected Abstracts from Symp on Organic Crystal Chemistry*, edited by Z. Kałuski, p. 70. UAM, Poznań, Poland.

Johnson, C. K. (1976) *ORTEP*II. Report ORNL-5138. Oak Ridge National Laboratory, Tennessee, USA.

Kozma, D., Böcskei, Z., Kassai, C., Simon, K. & Fogassy, E. (1996). *Chem. Commun.* pp. 753–754.

Kuma Diffraction (1991). *KM*-4 *User's Guide*, Version 3.2. Kuma Diffraction, Wrocław, Poland.

Kuma Diffraction (1999*a*). *KM*-4 *CCD Software*, Version 1.162. Kuma Diffraction Instruments GmbH, Wrocław, Poland.

Kuma Diffraction (1999*b*). *KM*-4 *RED Software*, Version 1.162. Kuma Diffraction Instruments GmbH, Wrocław, Poland.

Lehmann, M. S. & Larsen, F. K. (1974). *Acta Cryst.* A**30**, 580–584.

Motherwell, W. D. S., Shields, G. P. & Allen, F. H. (2000). *Acta Cryst.* B**56**, 857–871.

Rychlewska, U., Szarecka, A., Rychlewski, J. & Motała, R. (1999). *Acta Cryst.* B**55**, 617–625.

Rychlewska, U. & Warżajtis, B. (2000). *Acta Cryst.* B**56**, 833–848.

Rychlewska, U. & Warżajtis, B. (2001). *Acta Cryst.* B**57**, 415–427.

Rychlewska, U., Warżajtis, B., Hoffmann, M. & Rychlewski, J. (1997). *Molecules*, **2**, 106–113.

Sheldrick, G. M. (1990). *Acta Cryst.* A**46**, 467–473.

Sheldrick, G. M. (1997). *SHELXL*97. University of Göttingen, Germany.

Siemens (1989). *Stereochemical Workstation Operation Manual*, Release 3.4. Siemens Analytical X-ray Instruments Inc., Madison, Wisconsin, USA.

Szarecka, A., Hoffmann, M., Rychlewski, J. & Rychlewska, U. (1996). *J. Mol. Struct.* **374**, 363–372.

Szarecka, A., Rychlewska, U. & Rychlewski, J. (1999). *J. Mol. Struct.* **474**, 25–42.

Szarecka, A., Rychlewski, J. & Rychlewska, U. (2000). *Prog. Theoret. Chem. Phys.* **II**, 355–366.

Szczepańska, B., Gdaniec, M. & Rychlewska, U. (1995). *J. Incl. Phenom. Mol. Recogn. Chem.* **22**, 211–219.

Szczepańska, B. & Rychlewska, U. (1994). *Correlations, Transformations and Interactions in Organic Chemistry*, edited by D. W. Jones & A. Katrusiak, pp. 233–244. Oxford University Press.